MALAYSIAN JOURNAL OF SCIENCE
MJS
ISSN 1394-3065

Regular Issue

Malaysian Journal of Science 44 (3): 56-63 (September 2025) https://mjs.um.edu.my

Blue TiO_2 Nanotube (b-TiO_2) as a Support Material Electrode in a Photoelectrochemical Cell for Nitrogen Fixation

Muhammad Iqbal Syauqi[1a], Grandprix TM Kadja[2bcd] and Jarnuzi Gunlazuardi[3a*]

Abstract: We have been developing an artificial photosynthesis device based on a photoelectrochemical cell to convert N_2 to NH_3 in a greener way as an alternative to the Haber–Bosch process, which requires high energy and releases a huge amount of CO_2; this device consists of a dark cathode and photoanode. An electrode material that can absorb nitrogen and weaken its chemical bond is necessary for the dark cathode, while a photoanode material that can absorb visible light and have an intrinsic oxidation potential to split water is necessary. Currently, we are developing blue TiO_2 (b-TiO_2) and CoO_x modified b-TiO_2 for both electrode materials. b-TiO_2 was synthesized by the electrochemical reduction of TiO_2 nanotubes in aqueous solution, whereas TiO_2 nanotubes were prepared using the electro-oxidation technique. The synthesized b-TiO_2 exhibited a bandgap shift to 2.96 eV and an increase in conductivity owing to the presence of Ti^{3+} species. The addition of CoO_x to b-TiO_2 shifted the bandgap to 2.70 eV and increased its oxidative performance, as shown by the negative shift of the water oxidation onset potential and the 13.55% increase in RhB degradation under visible light and 500 mV external bias. Furthermore, when used in tandem as a dark cathode and photoanode, the device can convert N_2 to NH_3 up to 0.0063 µmol h^{-1} cm^{-1} without external bias and 0.0128 µmol h^{-1} cm^{-1} with 500 mV external bias.

Keywords: *Blue TiO_2; PEC Cell; N_2 Fixation; Artificial Photosynthesis.*

1. Introduction

N_2 fixation to ammonia is a relevant process from an industrial perspective because of the high demand for the product and the abundant and cheap resources. However, owing to the high activation energy required to break the N≡N bond, the direct utilization of N_2 for chemical synthesis is a difficult task (Keane et al. 2015). The only industrial way to fix nitrogen is the Haber–Bosch process, which produces ammonia from N_2 and H_2; it needs extreme conditions (450°C, 300 bar) and produces high CO_2 emission as the hydrogen source used in the reaction comes from burning fossil fuel (Falcone et al. 2018).

Recently, using photocatalytic and electrocatalytic pathways, it is possible to achieve N_2 to NH_3 conversion in ambient conditions (Ye et al. 2019). A catalyst that could selectively and efficiently absorb and weaken N≡N such as oxygen vacancy (OV) in the metal oxide (Hirakawa et al. 2017), metal nanoparticle (Zheng et al. 2019), or molecular catalyst (M. Li et al. 2018) is necessary for the process. The hydrogen source comes from H_2O; for the energy source, rather than thermal energy, electricity or photon energy is used to generate electrons and holes for the redox reactions of N_2 and H_2O to produce NH_3 (J. Yang et al. 2018).

Among all the photoelectrocatalysts, TiO_2 is one of the most popular materials developed because of its low toxicity, good chemical stability, low price, and superior photocatalytic activity. TiO_2 matrix contains a certain amount of OV and Ti^{3+} that could act as an active N_2 binding site so that the photocatalytic conversion of NH_3 can occur (Hirakawa et al. 2017; M. Li et al. 2018). However, many challenges remain for full-potential solar applications owing to TiO_2 high bandgap energy and high recombination rate (Gupta and Tripathi 2011). One of the ways to overcome this challenge is to perform self-doping reduction under suitable conditions to enhance Ti^{3+} and OV populations in TiO_2. The result will be blue-colored TiO_2 (b-TiO_2) with higher photoactivity in the visible light and infrared region, more Ti^{3+}/OV population, and far better conductivity than pristine TiO_2 (Ullattil et al. 2018; Yu, Nguyen, and Lee 2018) (G. Zhang et al. 2020). For example, in the electrolysis approach, Zhang et al. used a TiO_2 nanosheet on a Ti substrate as the cathode at 0.7 V vs. SHE. During electrocatalytic fixation, the Ti^{3+} and OVs, which act as N_2 active sites, are generated in situ on TiO_2, enabling N_2 to NH_3 conversion with a yield of 9.16 × 10^{-11} mol s^{-1} cm^{-2} (R. Zhang et al. 2018). In the photocatalysis technique, rutile TiO_2 with a surface defect was used by Hirakawa et al. to produce NH_3 from N_2 in UV light with a yield of 0.062 mg h^{-1} g^{-1} (Hirakawa et al. 2017). However, further improvements in the photocatalyst and electrocatalyst systems are required to enhance the conversion efficiency, selectivity, and durability to compete with the well-established Haber–Bosh process.

One of the strategies provided is using a photoelectrochemical

Authors information:
[a]Department of Chemistry, Faculty of Mathematics and Natural Sciences (FMIPA), Universitas Indonesia, Depok 16424, INDONESIA. E-mail: jarnuzi@ui.ac.id[3]
[b]Division of Inorganic and Physical Chemistry, Institut Teknologi Bandung, Jalan Ganesha no. 10, Bandung, 40132, INDONESIA.
[c]Research Center for Nanosciences and Nanotechnology, Institut Teknologi Bandung, Jl. Ganesha no. 10, Bandung, 40132, INDONESIA.
[d]Center for Catalysis and Reaction Engineering, Institut Teknologi Bandung, Jl. Ganesha no. 10, Bandung, 40132, INDONESIA.
*Corresponding Author: jarnuzi@ui.ac.id

Received: June, 2020
Accepted: September, 2021
Published: September, 2025

DOI:https//doi.org/10.22452/mjs.vol44no3.6
Malaysian Journal of Science 44(3): 56-63 (September 2025)

(PEC) cell that combines the privilege of photocatalysis (infinite source of light energy) with better charge separation during electrolysis. Moreover, cell efficiency could be further enhanced by coupling the PEC cell with the optimized PV cell (Ali et al. 2016). Generally, devices consist of a photocathode that absorbs N_2 while generating electrons in contact with a light source and a counter electrode that undergoes an oxidation reaction. For example, Li et al. reported that a PEC system constructed by TiO_2/Au/a-TiO_2 photocathode with a Pt counter electrode achieves 1.34×10^{-8} mol h^{-1} cm^{-2} NH_3 yield without external bias (C. Li et al. 2018). In another case, Ye et al. used a MoS_2@TiO_2 photocathode with an external bias of 0.3 V vs. RHE to convert N_2 to NH_3 with an excellent yield of 1.42×10^{-6} mol h^{-1} cm^{-2} (Ye et al. 2019).

However, despite its enormous potential, the work of N_2 fixation using PEC systems has rarely been explored. In an attempt to explore the potential of b-TiO_2 as a support material electrode in a PEC system, we constructed a PEC system with a different construction with a common PEC N_2 reduction cell. By altering the b-TiO_2 nanostructure to a nanotube form, the materials will have a higher surface area and better electron transport owing to their porous 2D channeling electron properties (Kang et al. 2008); thus, they are projected to be good base electrodes in PEC systems for N_2 reduction. Two b-TiO_2 nanotubes will be used in tandem as the dark cathode and photoanode in PEC cells. Inspired by photosynthesis phenomena, the light reaction is for water oxidation at the photoanode, while the reduction reaction is protected from light and undergoes pure electrochemical reduction. In this way, the materials used can be more varied as the risk of N_2 catalyst to degrade by photoreaction decreases. As a photoanode, the oxidative properties of b-TiO_2 should be highlighted as it will oxidize the water to produce electrons and H^+ ions as materials for NH_3 production. Thus, we introduced CoOx species as a co-catalyst to enhance the photooxidation properties of b-TiO_2 (Ramakrishnan et al. 2016; Y. Yang et al. 2018). Furthermore, the electron that is gained by the photoanode will be transferred via an external circuit to b-TiO_2 at the dark cathode, which was exposed by N_2 gas, whereas upon absorption a conversion of N_2 gas to ammonia occurred.

2. Materials and Methods

Materials

Titanium sheets (99.78% pure) were obtained from Sigma-Aldrich. Ethylene glycol, ethanol, methanol, sodium sulfate, hydrofluoric acid, nitric acid, NH_4F, $Co(NO_3)_2.2H_2O$, and rhodamine-B were obtained from Merck Millipore. Deionized water (Millipore analytical grade) was used in almost all the experiments.

Preparation of Blue TiO_2 Based Electrodes

The titanium sheet was anodized at a distance of 1.5 cm vs. the stainless steel electrode in an ethylene glycol solution containing NH_4F (0.3% wt.) and H_2O (2% v) under a constant potential of 40 V at room temperature (25°C). After 45 min, the as-anodized TiO_2 was cleaned with deionized water, dried in open air, and calcined at 450°C for 2 h in air. The synthesis of b-TiO_2 was carried out by the electrochemical reduction of annealed TiO_2 at 1.5 V vs. Ag/AgCl in Na_2SO_4 0.1 M solution for a certain time (20, 40, and 60 min). To enhance the photoactivity at the anode, the sample with the optimum reduction time was doped with CoO_x using the photodeposition method. The synthesized b-TiO_2 was dipped in 0.01 M $Co(NO_3)_2$ in methanol solution for 2 h and then exposed to UV light for another 2 h. The samples were then characterized in an electrochemical working station. The morphologies of the samples were examined by SEM. The crystalline phase was determined by XRD (SHIMADZU XRD-6100) with Cu K □ radiation (λ = 0.15406 nm) at 40 kV and 30 mA. UV–Visible (UV–Vis) diffuse reflectance spectroscopy of the electrodes was carried out using a spectrophotometer (Agilent) with $BaSO_4$ as the standard. In this work, we evaluated the performance of b-TiO_2 as a dark cathode for nitrogen fixation and as a photoanode for dye degradation.

Activity Test of b-TiO_2 as a Photoanode

The degradation of RhB in an aqueous solution with a concentration of 10 mg/L (25 mL solution with 0.1 M Na_2SO_4 as a supporting electrolyte) in a quartz reactor was used to evaluate the PEC performance of the anodes. The blue TiO_2 anode and Pt rod cathode were immersed in the solution at a distance of 1.5 cm. The degradation was conducted using a halogen lamp as a light source under 0.5 V external bias (vs. Ag/AgCl) and continuous stirring. A UV–Vis spectrophotometer (UV–Thermo-Scientific) was used to measure the absorbance of the solution and the degradation rate of RhB. For comparison, the degradation due to photolysis and external bias addition was determined using the same apparatus but with stainless steel as the anode.

Ammonia Evolution Measurement by a PEC Cell

The activity of the PEC cell was determined by the cell's ability to convert nitrogen to ammonia. The photoanode and dark cathode were placed in an H-type quartz reactor, as depicted in Figure S1. The cathode and anode chambers were separated using a Nafion membrane containing 75 mL Na_2SO_4 0.1 M solution in both chambers. The b-TiO_2 electrode for the dark cathode was connected to the negative pole of the power supply, while the b-TiO_2/CoO_x photoanode was connected to the positive pole. Before the reaction, the system was bubbled with N_2 flow (100 mL/min) for 30 min to remove the dissolved air from the solution. During the reaction, the photoanode was exposed to a halogen lamp with an intensity of 30000 lux, whereas the dark cathode was protected from light exposure and was exposed to high-purity N_2 gas, at 100 mL/min flow rate. The chamber of the H-type reactor, which contained the dark cathode, was connected to a chamber containing 0.01 M HCl as the ammonia absorber. An aliquot of the reaction solution and HCl as NH_3 absorber was taken out after the 4-h reaction. As a comparison, we prepared a reaction control performed under the same conditions but without light exposure. Furthermore, we performed another comparison by introducing a 500-mV external bias to the system while the photoreaction occurred (photoelectrofixation). The ammonia concentration was determined using the phenate

DOI:https//doi.org/10.22452/mjs.vol44no3.6
Malaysian Journal of Science 44(3): 56-63 (September 2025)

method, in which 5 mL aliquots were reacted with 200 µL phenol solution, 20 µL sodium nitroprusside, and 500 µL of NaOCl. The mixture was rested for 2 h before being measured with a UV–Vis spectrophotometer at 640 nm.

3. Results and Discussion

Synthesis of Blue TiO_2 Nanotube Arrays (b-TiO_2)

The preparation of the b-TiO_2 electrode consisted of two steps: synthesis of TiO_2 nanotube arrays by anodization of the titanium sheet followed by calcination and electrochemical reduction of the TiO_2 nanotube arrays to obtain b-TiO_2. The profile of the anodization current density over time shows a typical profile that leads to the formation of the nanotube morphology of TiO_2, consisting of three stages of current change (Figure 1a): the first stage (I) is the formation of a compact oxide layer, which is indicated by the sudden drop of the current density in the system. The second stage (II) is the dissolution of the oxide layer, which creates a hole that later dips to form tube arrays. The current density profile in this stage was indicated by increasing the current until at a certain time; a steady current density was observed. The steady current density belongs to the third stage (III) in which the reaction between dissolution and formation of TiO_2 reaches equilibrium; this stage determines the tube length. This current density profile of the nanotube array formation was confirmed by the obtained SEM image (Figure 3a), which shows that the nanotube morphology was observed with a diameter of 57.53 ± 8.33 nm and tube length of 4.13 µm. After being calcined at 450°C for 2 h., the obtained gray TiO_2 nanotube arrays were subjected to electrochemical reduction for 40 min to obtain blue TiO_2.

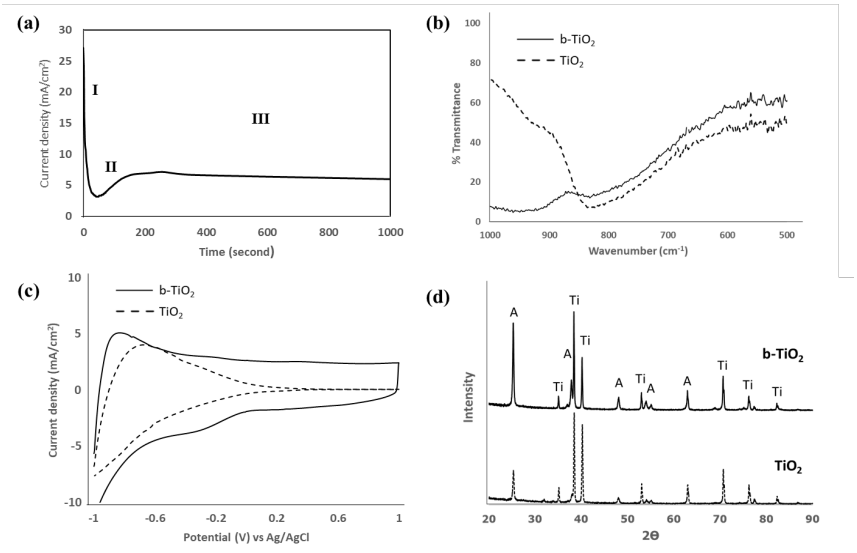

Figure 1. Current density profiles of the anodization process (a), material characterizations by FTIR (b), cyclic voltammetry in Na_2SO_4 0.1M (100 mV s^{-1} vs. Ag/AgCl) (c), and XRD (d).

Reducing TiO_2 electrochemically generates an OV, which can be ascribed to the decrease in the intensity of the Ti-O-Ti peak at 850–720 cm^{-1} in FTIR measurement (Figure 1b). The reduction process also gives the exact difference in the cyclic voltammetry profiles of TiO_2 and b-TiO_2. As shown in Figure 1c, TiO_2 exhibits high resistance at a high potential, leading to a low current; hence, the curve exhibits a pinched shape. b-TiO_2 exhibited capacitive curves with rectangular shapes. The difference is due to the increase in conductivity, which can be attributed to the trapped electrons at Ti^{3+} sites generated by cathodic polarization (Zhu et al. 2018).

The XRD measurements, as shown in Figure 1d, indicated that there was no significant change in the XRD pattern after reduction. The sample was in good agreement with anatase TiO_2 (JCPDS, PDF 84-1286), indicating that the electrochemical reduction did not change the crystal phase, which is consistent with previous reports (Kim et al. 2016; H. Li et al. 2014; Zhu et al. 2018).

When electrochemically reduced, the gray TiO_2 became black, indicating the formation of Ti^{3+}. However, immediately after the electrochemical reduction stopped, the black color gradually disappeared until it reached an equilibrium state where the color of TiO_2 became blue (Figure 2a). This might be caused by the re-oxidation of some Ti^{3+} sites when they come into contact with oxygen in the air (Kim et al. 2016).

DOI:https//doi.org/10.22452/mjs.vol44no3.6
Malaysian Journal of Science 44(3): 56-63 (September 2025)

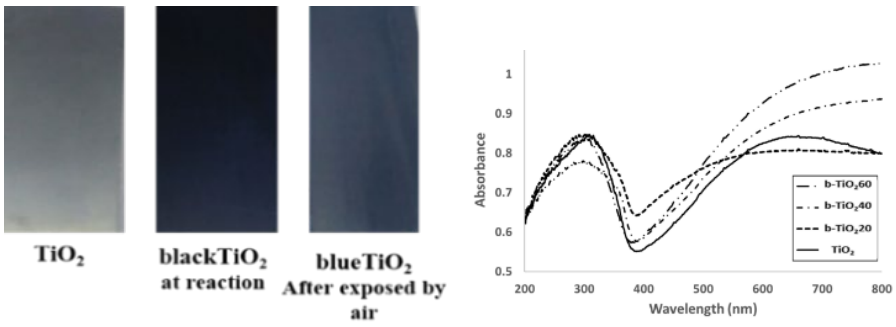

Figure 2. Pictures of bare TiO_2, black TiO_2, and b-TiO_2 electrodes (a) and UV–Vis DRS spectrum of TiO_2 and b-TiO_2 with various reduction times (b).

The presence of Ti^{3+} (defect oxygen) in TiO_2 will increase the conductivity and photocatalytic activity in the visible light region; however, too much defect will decrease the activity owing to the formation of electron recombination sites and the possibility of destroying the crystal morphology (Hong et al. 2019). To optimize the Ti^{3+} population in b-TiO_2, the reduction times of 20, 40, and 60 min were varied. Figure 2b shows the absorbance profile of each sample analyzed by the UV–Vis DRS. Pristine and blue TiO_2 exhibit intrinsic absorption at wavelengths below 400 nm. The visible light absorption of TiO_2 may be caused by light scattering because of pores or cracks in the nanotube arrays (Zhu et al. 2018). The reduction treatment generally gives a slight decrease in the UV region absorption, resulting in the enhancement of visible light absorption. To study more about the effect of reduction time on the photoactivity of b-TiO_2, the photocurrents in both the UV and VIS regions were measured by employing a three-electrode system cell, where TiO_2, Pt rod, and Ag/AgCl were used as the working, counter, and reference electrodes, respectively, in 0.1 M Na_2SO_4 electrolyte. As shown in Table 1, the reduction resulted in a redshift effect in the bandgap from 3.23 eV to approximately 3.00 eV. There is no significant difference in the bandgap shift and photocurrent with the length of the reduction time, indicating that there is a limitation for the deposition of Ti^{3+} in the anatase phase using the cathodic process (Hong et al. 2019; Kim et al. 2016; Zhu et al. 2018).

The photocurrent in the visible region increased with the reduction time, reaching a maximum at 40 min and decreasing at 60 min reduction, whereas photocurrent in the UV region decreased. This phenomenon can be ascribed to the increasing of Ti^{3+} population that leads to a narrower bandgap, thereby resulting in a visible light shift of its activity over time reaching its maximum at 40 min and reduction becoming excessive at 60 min reduction time. The decrease in photocurrent in the UV region may also be caused by the distorted tube morphology and the generated OV owing to the excessive reduction process. As shown in SEM observation in Table 1 and Figure 3, the reduction time generally did not change the morphology; however, it was observed that cathodic exposure under a given condition decreased the tube diameter, which can be clearly observed at the 60-min reduction time. This finding agrees with a previous report on excessive electrochemical reduction leading to morphological distortion (Zhou and Zhang 2014). This observation may have caused the decrease in photocurrent in the UV region, besides the increase in the Ti^{3+} population; it also explains the abnormally high absorption of b-TiO_2 observed in the visible region spectrum (Figure 2b), which might not be caused by light absorption but also by the scattering effect. Regardless of the result, for the next application of b-TiO_2, we used a 40-min reduction time because it gave the highest photocurrent in the visible region, the lowest bandgap, and the minimum morphological change.

Table 1. Effect of time reduction on the properties of b-TiO2

Sample	TiO_2 reduction time (min)	Bandgap (eV)	Photocurrent UV (μA/cm^2)	Photocurrent VIS (μA/cm^2)	Tube diameter (nm)	Tube length (μm)
TiO_2	0	3.25	15.25	0.88	57.53 ± 8.33	4.13
b-TiO_2 20	20	2.97	13.32	1.26	56.22 ± 12.83	4.15
b-TiO_2 40	40	2.96	12.50	1.46	54.67 ± 12.12	4.12
b-TiO_2 60	60	3.02	11.77	1.36	48.50 ± 13.80	4.13

DOI:https//doi.org/10.22452/mjs.vol44no3.6
Malaysian Journal of Science 44(3): 56-63 (September 2025)

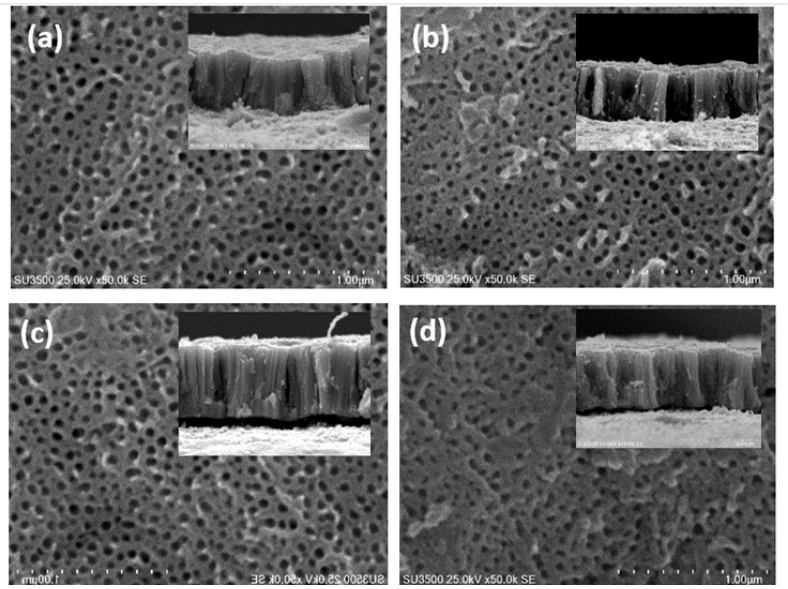

Figure 3. SEM images of pristine TiO_2 nanotube arrays (a) and b-TiO_2 with 20 min (b), 40 min (c), and 60 min (d) reduction times. The inset shows a cross-section of each sample.

Characterization and Activity Test of b-TiO_2/CoO_x Photoanode

To enhance the electrode's ability as a photoanode material, we introduced CoO_x species using a photodeposition method. Figure S2 shows that the XRD pattern of the b-TiO_2/CoO_x sample did not show the CoO_x peak; this indicates that the amount of cobalt deposited was less than 7% wt (Amer, Ghanem, and Arunachalam 2019). Nevertheless, the presence of cobalt in the sample can be determined by FTIR measurements and indicates the bandgap calculation results. The Tauc Plot of b-TiO_2/CoO_x (Figure 4a) shows two bandgaps: 3.00 eV and 2.70 eV, which correspond to b-TiO_2 and CoO_x species, respectively. Furthermore, the FTIR measurements show absorption peaks at approximately 525, 575, 650, and 680 cm^{-1} that are ascribed to the occurrence of Co_3O_4 species (Y. Li et al. 2016) (Tang, Wang, and Chien 2008).

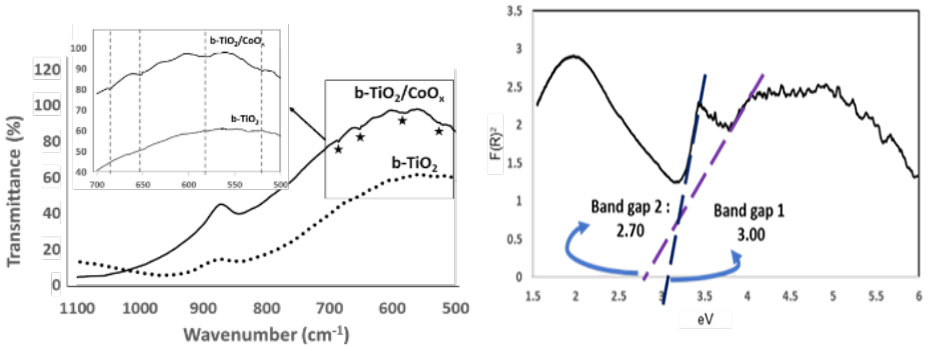

Figure 4. Characterization of b-TiO_2/CoO_x by Tauc Plot (a) and FTIR (b)

The ability of the synthesized materials to oxidize water and to degrade organic dye using RhB as a model compound was examined. Figure 5a shows the anodic linear sweep voltammetry results for each sample in an aqueous solution from 0 V to 2 V with a scan rate of 100 mV s^{-1}. It is observed that introducing Ti^{3+} and CoO_x to TiO_2 could shift the onset potential of water oxidation closer to zero, indicating that water oxidation becomes easier in the presence of Ti^{3+} and CoO_x (Y. Yang et al. 2018). Figure 5b shows the RhB degradation rate under a 500-mV external bias potential. With an 80-min degradation time, photoelectrolysis using a stainless steel electrode contributed to 5% of the dye degradation, whereas TiO_2, b-TiO_2, and b-TiO_2/CoO_x degraded RhB at 29.1%, 40.2%, and 46.5%, respectively. This result indicates that introducing Ti^{3+} to TiO_2 matrix can increase the degradation performance by 27.61%, while CoO_x addition adds 13.55% more from b-TiO_2. This result is in agreement with previous research (Ramakrishnan et al. 2016; Ullattil et al. 2018; Y. Yang et al. 2018), which reported that introducing Ti^{3+} and CoO_x to TiO_2 could greatly increase the photoanode activity.

DOI:https//doi.org/10.22452/mjs.vol44no3.6
Malaysian Journal of Science 44(3): 56-63 (September 2025)

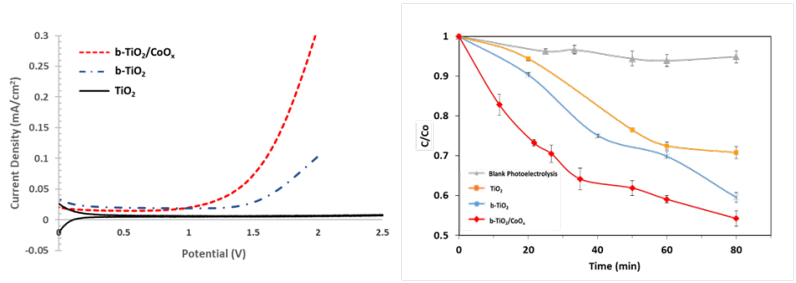

Figure 5. Anodic linear sweep voltammetry to determine the onset potential for water oxidation: 0.1 M Na_2SO_4, Pt Rod vs. Ag/AgCl (a). RhB degradation rate at different electrodes (b).

Photoelectrochemical Cell Performance Measurements

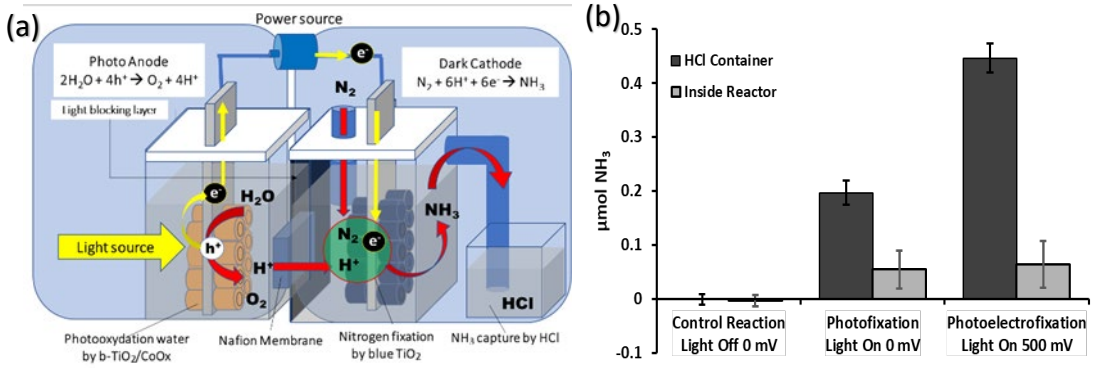

Figure 6. Schematic diagram of the PEC system (a). Result of nitrogen fixation after 4 h (b).

Figure 6a shows a schematic diagram of the PEC cell used in the experiments. Two chambers separated by a Nafion membrane were used with 10 cm^2 surface area electrodes. When the light was turned on, the electrons on the b-TiO_2/CoO_x photoanode were excited to the TiO_2 conduction band and then transferred to the dark cathode by the external circuit. The migrated electron leaves a hole (h^+) on the surface of the photoanode; this hole oxidizes water to produce oxygen and protons. The generated protons migrate through the Nafion membrane to find a dark cathode. Then, when the electron and proton from the photoanode meet the "activated nitrogen" on b-TiO_2, the conversion of N_2 to NH_3 occurs. The OV in b-TiO_2 can absorb and activate the strong N≡N bonding to the hydrazine intermediate, which leads to easier breaking of the bonding, resulting in a conversion reaction (Hirakawa et al. 2017; M. Li et al. 2018).

As shown in Figure 6a, the ammonia production process was conducted in the HCl solution container and reactor solution chamber. The results in Figure 6b shows that NH_3 detected in the reactor under photofixation and photoelectrofixation experimental conditions was low compared to the results in the HCl chamber; this means that the majority of NH_3 generated was transferred to the HCl container via N_2 bubbling. In the HCl solution chamber, no NH_3 was detected when no light or bias potential was provided. However, a substantial amount of NH_3 was detected (total 0.2509 µmol NH_3 after 4 h reaction) when the light was turned on under a 0 mV bias potential, equal to 0.0063 µmol h^{-1} cm^{-1}. To ensure that the detected NH_3 was from the reaction, the NH_3 concentration from the control (light off with no bias) was measured. The result showed that NH_3 detected was below the detection limit, indicating that the reaction indeed originated from N_2 fixation. Furthermore, the addition of 500 mV external potential gave a better result with 0.5104 µmol NH_3 generated after 4 h, equal to 0.0128 µmol h^{-1} cm^{-1}. This result proves that adding power to the system can lead to a higher NH_3 result. The external potential increased the kinetics of the reaction by providing more electrons to the cathode site (T. Li et al. 2017).

Compared with other works, as shown in Table S1, this work is inferior. This may be owing to the photoanode ability, which has not yet reached the optimum composition. However, the potential to further improve this device is still vast. By further optimizing the dark cathode's Ti^{3+}/OV population, the photoanode's ability to perform photooxidation, and the external bias input, this device can still be improved. In future applications, instead of using electricity, employing solar cells as a natural power provider will be a better approach so that this system can operate without any electrical source.

4. Conclusion

Blue TiO_2 nanotubes synthesized by self-doping electrochemical reduction in an aqueous Na_2SO_4 solution have better conductivity and visible light activity than pristine TiO_2. The introduction of the CoO_x species into b-TiO_2 was successful and resulted in the

DOI:https//doi.org/10.22452/mjs.vol44no3.6
Malaysian Journal of Science 44(3): 56-63 (September 2025)

formation of Co_3O_4, thus creating a more powerful oxidation catalyst matrix. This was demonstrated by the negative shifting of the water oxidation onset potential and the enhancement of RhB degradation, which reached 46.5% in only 80 min. The combination of b-TiO_2/CoO_x as the photoanode and b-TiO_2 as the dark cathode in the PEC cell resulted in the conversion of N_2 to NH_3. With a 10 cm^2 electrode area, just by the electron supplied from the photoanode, the system gives 0.2509 µmol NH_3 after a 4-h reaction. The addition of 500 mV external bias gives a better result under the same reaction conditions; the addition of external potential gives 0.5104 µmol NH_3. This result shows that blue TiO_2 has great potential as an electrode in PEC artificial photosynthesis cells for nitrogen fixation to ammonia.

5. Acknowledgement

The authors would like to thank Universitas Indonesia, SDID-RISTEK-DIKTI, for funding this research through the Scholarship of PMDSU Batch IV Scheme (2018–2019); PMDSU research grant scheme (2019); and partly PDUPT research grant scheme (2019), PMDSU (2025). MIS wrote the English manuscript on technical detail, GPTM took care of the reliability of this research and manuscript, and JG supervised this research and gave a critical suggestion on the research pipeline. All authors have checked and approved the final manuscript.

5. References

Ali, Muataz et al. 2016. "Nanostructured Photoelectrochemical Solar Cell for Nitrogen Reduction Using Plasmon-Enhanced Black Silicon." *Nature Communications* 7: 11335.

Amer, Mabrook S., Mohamed A. Ghanem, and Prabhakarn Arunachalam. 2019. "Mesoporous Titanium Dioxide Modified with Cobalt." *Catalysts* 9(10).

Falcone, Marta et al. 2019. "The Role of Bridging Ligands in Dinitrogen Reduction and Functionalization by Uranium Multimetallic Complexes." *Nature Chemistry* 11(2): 154–60.

Gupta, Shipra Mital, and Manoj Tripathi. 2011. "A Review of TiO_2 Nanoparticles." *Chinese Science Bulletin* 56(16): 1639–57. http://link.springer.com/10.1007/s11434-011-4476-1.

Hirakawa, Hiroaki, Masaki Hashimoto, Yasuhiro Shiraishi, and Takayuki Hirai. 2017. "Photocatalytic Conversion of Nitrogen to Ammonia with Water on Surface Oxygen Vacancies of Titanium Dioxide." *Journal of the American Chemical Society* 139(31): 10929–36.

Hong, Sung Pil, Seonghwan Kim, Nayeong Kim, Jeyong Yoon, and Choonsoo Kim. 2019. "A Short Review on Electrochemically Self-Doped TiO_2 Nanotube Arrays: Synthesis and Applications." *Korean Journal of Chemical Engineering* 36(11): 1753–66.

Kang, Soon Hyung, Jae Yup Kim, Hyun Sik Kim, and Yung Eun Sung. 2008. "Formation and Mechanistic Study of Self-Ordered TiO_2 Nanotubes on Ti Substrate." *Journal of Industrial and Engineering Chemistry* 14(1): 52–9.

Keane, Andrew J., Wesley S. Farrell, Brendan L. Yonke, Peter Y. Zavalij, and Lawrence R. Sita. 2015. "Metal-Mediated Production of Isocyanates, Isocyanates, R3EN=C=Ofrom Dinitrogen, Carbon Dioxide, and R3ECl." *Angewandte Chemie* 54(35): 10220–24.

Kim, Choonsoo, Seonghwan Kim, Sung Pil Hong, Jaehan Lee, and Jeyong Yoon. 2016. "Effect of Doping Level of Colored TiO_2 Nanotube Arrays Fabricated by Electrochemical Self-Doping on Electrochemical Properties." *Physical Chemistry Chemical Physics* 18(21): 14370–75.

Li, Chengcheng et al. 2018. "Promoted Fixation of Molecular Nitrogen with Surface Oxygen Vacancies on Plasmon-Enhanced TiO_2 Photoelectrodes." *Angewandte Chemie* 57(19): 5278–82.

Li, Hui et al. 2014. "Electrochemical Doping of Anatase TiO_2 in Organic Electrolytes for High-Performance Supercapacitors and Photocatalysts." *J. Mater. Chem. A* 2(1): 229–36.

Li, Mengqiao et al. 2019. "Recent Progress on Electrocatalyst and Photocatalyst Design for Nitrogen Reduction." *Small Methods* 3(6): 1800388. http://doi.wiley.com/10.1002/smtd.201800388.

Li, Tengfei et al. 2017. "Photoelectrochemical Oxidation of Organic Substrates in Organic Media." *Nature Communications* 8(1): 390.

Li, Yang et al. 2016. "Identification of Cobalt Oxides with Raman Scattering and Fourier Transform Infrared Spectroscopy." *Journal of Physical Chemistry C* 120(8): 4511–16.

Ramakrishnan, Vivek, Hyun Kim, Jucheol Park, and Beelyong Yang. 2016. "Cobalt Oxide Nanoparticles on TiO_2nanorod/FTO as a Photoanode with Enhanced Visible Light Sensitization." *RSC Advances* 6(12): 9789–95.

Tang, Chih Wei, Chen Bin Wang, and Shu Hua Chien. 2008. "Characterization of Cobalt Oxides Studied by FT-IR, Raman, TPR and TG-MS." *Thermochimica Acta* 473(1–2): 68–73.

Ullattil, Sanjay Gopal, Soumya B. Narendranath, Suresh C. Pillai, and Pradeepan Periyat. 2018. "Black TiO_2 Nanomaterials: A Review of Recent Advances." *Chemical Engineering Journal* 343(January): 708–36.

DOI:https//doi.org/10.22452/mjs.vol44no3.6
Malaysian Journal of Science 44(3): 56-63 (September 2025)

Yang, Jianhua, Yanzhen Guo, Wenzheng Lu, Ruibin Jiang, and Jianfang Wang. 2018a. "Emerging Applications of Plasmons in Driving CO_2 Reduction and N2 Fixation." *Advanced Materials* 30(48): e1802227.

Yang, Yang et al. 2018b. "Cobalt-Doped Black TiO_2 Nanotube Array as a Stable Anode for Oxygen Evolution and Electrochemical Wastewater Treatment." *ACS Catalysis* 8(5): 4278–87.

Ye, Wen et al. 2019. "Efficient Photoelectrochemical Route for the Ambient Reduction of N_2 to NH_3 Based on Nanojunctions Assembled from MoS_2 Nanosheets and TiO_2." *ACS Applied Materials and Interfaces* 11(32): 28809–17.

Yu, Jianmin, Chau Thi Kim Nguyen, and Hyoyoung Lee. 2018. "Preparation of Blue TiO_2 for Visible-Light-Driven Photocatalysis" *Titanium Dioxide – Material for a Sustainable Environment*. (edited by: D Yang). InTech.

Zhang, Guoqiang, Xun Yang, Chuanxin He, Peixin Zhang, and Hongwei Mi. 2020. "Constructing a Tunable Defect Structure in TiO_2 for Photocatalytic Nitrogen Fixation." *Journal of Materials Chemistry A* 8(1): 334–41.

Zhang, Rong et al. 2018. "Enabling Effective Electrocatalytic N_2 Conversion to NH_3 by the TiO_2 Nanosheets Array under Ambient Conditions." *ACS Applied Materials and Interfaces* 10(34): 28251–55.

Zheng, Jianyun et al. 2019. "Photoelectrochemical Synthesis of Ammonia on the Aerophilic-Hydrophilic Heterostructure with 37.8% Efficiency." *Chem* 5(3): 617–33.

Zhou, He, and Yanrong Zhang. 2014. "Electrochemically Self-Doped TiO_2 Nanotube Arrays for Supercapacitors." *Journal of Physical Chemistry C* 118(11): 5626–36.

Zhu, Liyan et al. 2018. "Black TiO_2 Nanotube Arrays Fabricated by Electrochemical Self-Doping and Their Photoelectrochemical Performance." *RSC Advances* 8(34): 18992–9000.

DOI:https//doi.org/10.22452/mjs.vol44no3.6
Malaysian Journal of Science 44(3): 56-63 (September 2025)